Contemporary Mathematics
Volume **586**, 2013
http://dx.doi.org/10.1090/conm/586/11633

Immersed finite element method of lines for moving interface problems with nonhomogeneous flux jump

Tao Lin, Yanping Lin, and Xu Zhang

Abstract. This article presents an immersed finite element method of lines for solving parabolic moving interface problems with a non-homogeneous flux jump. The immersed finite elements are used for spatial discretization, which allow the material interface to be embedded in the interior of elements in the mesh. This feature makes it possible to employ the method of lines for solving a moving interface problem over a fixed solution mesh. Numerical experiments are provided to show features of this new method.

1. Introduction

We consider the following parabolic moving interface problem:

$$\begin{cases} u_t - (\beta u_x)_x = f(t,x), & x \in \Omega,\ t \in (0, T_{end}], \\ u(t,x) = g(t,x), & x \in \partial\Omega,\ t \in (0, T_{end}], \\ u(0,x) = u_0(x), & x \in \overline{\Omega}. \end{cases} \tag{1.1}$$

Here $\Omega \subset \mathbb{R}$ is an open interval, and for the sake of simplicity, we assume that there is only one interface point $\alpha(t)$ moving inside Ω. This point separates Ω into two sub-intervals $\Omega^-(t)$ and $\Omega^+(t)$ such that $\Omega = \Omega^-(t) \cup \Omega^+(t) \cup \{\alpha(t)\}$ with $\Omega^-(t)$ on the left hand side of $\alpha(t)$. The diffusivity coefficient $\beta(t,x)$ is discontinuous across the interface $\alpha(t)$. Without loss of generality, we assume that it is a piece-wise constant function defined as follows:

$$\beta(t,x) = \begin{cases} \beta^-, & x \in \Omega^-(t), \\ \beta^+, & x \in \Omega^+(t). \end{cases} \tag{1.2}$$

Consequently, the solution u is assumed to satisfy the following nonhomogeneous interface jump conditions:

$$[u]|_{\alpha(t)} = 0, \tag{1.3}$$

$$[\beta u_x]|_{\alpha(t)} = Q(t). \tag{1.4}$$

2010 *Mathematics Subject Classification.* Primary 65M20, 65M60; Secondary 35R05.

Key words and phrases. Immersed finite element, method of lines, moving interface, nonhomogeneous.

This work is partially supported by NSF grant DMS-1016313, GRF grant of Hong Kong (Project No. PolyU 501709), AMA-JRI of PolyU, Polyu grant No. 5020/10P and NSERC (Canada).

The model problem (1.1)-(1.4) appears in many applications, for instance, the Stefan problem [**CDH67**] for simulating temperature distribution undergoing a phase transition such as ice melting into water. The well-known Stefan condition requires the flux jump to be proportional to the velocity of the moving front, which is nonzero in general. Other interesting applications include the simulation of the electric potential [**Coo75**], the modeling of the water flow in porous media with a source at the interface [**Miy06**], and the modeling of air-vapor-heat transport through textile materials [**ZS11**], to name just a few.

It is well known that finite element (FE) methods can be used for solving interface problems provided that solution meshes are aligned with the material interfaces. Consequently, each element in a mesh contains essentially only one type of materials. However, the basis functions on each element are generic polynomials independent of the interface jump conditions. The recently developed immersed finite element (IFE) methods [**LLW03, LLLR04, GLL07, AL09, He09, HLL11, WLL11, XLQ11, WWY12**] employ an alternative approach to solve interface problems. IFE methods can use meshes independent of the interface location, but their basis functions are specially constructed to satisfy pertinent interface jump conditions.

For moving interface problems, using IFEs in spatial discretization has a major advantage over traditional FEs in the sense that a fixed mesh can be used throughout the whole simulation so that popular methods such as the method of lines (MoL) can be employed to reduce a moving interface problem to an ordinary differential equation (ODE) system that can be solved numerically by a preferred ODE solver. Fully discrete Crank-Nicolson type IFE schemes [**HLLZ12**] and the IFE MoL [**LLZ12**] have been developed for solving moving interface problems with a homogeneous flux jump, *i.e.*, $Q(t) = 0$. In this article, we extend IFE MoL to problems with a nonhomogeneous flux jump.

The rest of this article is organized as follows. In Section 2, we develop an IFE MoL based on a semi-discrete formulation using linear IFEs. In Section 3, we present several numeral results to demonstrate features of this new scheme. Brief conclusions are summarized in Section 4.

2. IFE Method of Lines

2.1. Linear IFE Functions for Nonhomogeneous Flux Jump. Let $\mathcal{T}_h$ be a uniform partition of Ω with a mesh size h. An element in this mesh is an interface element if $\alpha(t)$ is in its interior. Let $\mathcal{T}_h^{i,t}$, and $\mathcal{T}_h^{n,t}$ be the collections of interface elements and non-interface elements at time t, respectively. Also let $\mathcal{N}_h$ be the set of nodes in $\mathcal{T}_h$.

We use $\phi_j^t(x)$ to denote the global linear IFE basis function [**AL09**] associated with the node $x_j \in \mathcal{N}_h$. The superscript t on the basis function emphasizes the fact that it is either a linear IFE basis function or a standard linear FE basis function depending on whether $\alpha(t)$ is in the elements adjacent to the node x_j. Since $\alpha(t)$ changes with respect to time, $\phi_j^t(x)$ is time dependent even though the mesh is time independent [**HLLZ12**]. Then, we let $S_h^t(\Omega) = \text{span}\{\phi_j^t : x_j \in \mathcal{N}_h\}$ be the linear IFE space at the time t defined on the mesh $\mathcal{T}_h$. Note that in [**HLL11**], the authors enriched the IFE space by introducing an additional IFE function in order to handle the nonhomogeneous flux jump for elliptic interface problems. Our effort here is to extend this idea to the moving interface problem (1.1)-(1.4).

Assume, at time t, the interface point $\alpha(t)$ moves into the element $T = (x_j, x_{j+1})$, *i.e.*, T becomes an interface element such that $\alpha(t)$ separates T into $T^- = (x_j, \alpha)$, and $T^+ = (\alpha, x_{j+1})$. We construct an enrichment linear IFE function $\phi_J^t(x)$ for treating the nonhomogeneous flux jump as follow [**HLL11**]:

$$\phi_J^t(x) = \begin{cases} c_1(t)(x - x_j), & \text{for } x \in T^-, \\ c_2(t)(x_{j+1} - x), & \text{for } x \in T^+, \\ 0, & \text{otherwise.} \end{cases} \tag{2.1}$$

Note that ϕ_J^t is also time dependent, and $c_1(t)$, and $c_2(t)$ are determined by the following nonhomogeneous interface jump conditions

$$[\phi_J^t(\alpha)] = 0, \text{ and } [\beta \phi_{J,x}^t(\alpha)] = 1.$$

It is easy to show that $c_1(t)$ and $c_2(t)$ are uniquely determined by these conditions with the following formulas,

$$c_1(t) = \frac{x_{i+1} - \alpha}{\beta^-(\alpha - x_{i+1}) + \beta^+(x_i - \alpha)}, \quad c_2(t) = \frac{\alpha - x_i}{\beta^-(\alpha - x_{i+1}) + \beta^+(x_i - \alpha)}. \tag{2.2}$$

2.2. An IFE Method of Lines. We note that each IFE basis function $\phi_j^t(x)$ is associated with a fixed node $x_j \in \mathcal{N}_h$ even though $\phi_j^t(x)$ may changes with respect to t. Therefore, following the basic idea of the method of lines, we can look for a semi-discrete IFE solution to the moving interface problem in the following form:

$$u_h(t, x) = \tilde{u}_h(t, x) + \sum_{T \in \mathcal{T}_h^{i,t}} Q(t) \phi_J^t(x), \tag{2.3}$$

where $\tilde{u}_h(t, \cdot) \in S_h^t(\Omega)$ is the homogenized solution such that

$$\tilde{u}_h(t, x) = \sum_{x_j \in \mathcal{N}_h} u_j(t) \phi_j^t(x). \tag{2.4}$$

First, it is easy to see that $u_h(t, x)$ satisfies the jump conditions (1.3) and (1.4). Then, we determine the unknown coefficients $u_j(t)$ through a set of ODEs in t. Consider the weak form of the problem. Multiply $v \in H_0^1(\Omega)$ on both side of (1.1) and integrate on each Ω^s, $s = +, -$:

$$\int_{\Omega^s} u_t v \mathrm{d}x + \int_{\Omega^s} (\beta u_x)_x v \mathrm{d}x = \int_{\Omega} f v \mathrm{d}x, \ \forall\ v \in H_0^1(\Omega),$$

Applying integration by parts, summing over $s = +, -$, and using the relation (1.4), we obtain the following weak form:

$$\sum_{T \in \mathcal{T}_h} \int_T u_t v \mathrm{d}x + \sum_{T \in \mathcal{T}_h} \int_T \beta u_x v_x \mathrm{d}x = \int_{\Omega} f v \mathrm{d}x - Q(\alpha) v(\alpha), \ \forall\ v \in H_0^1(\Omega).$$

This weak form suggests the following IFE equations for determining $u_h \in S_h^t(\Omega)$:

$$\sum_{T \in \mathcal{T}_h} \int_T \frac{\partial u_h}{\partial t} v_h \mathrm{d}x + \sum_{T \in \mathcal{T}_h} \int_T \beta u_{hx} v_{hx} \mathrm{d}x = \int_{\Omega} f v_h \mathrm{d}x - Q(\alpha) v_h(\alpha), \ \forall\ v_h \in S_h^{t,0}(\Omega),$$

where $S_h^{t,0}(\Omega) = \{\phi_j \in S_h^t(\Omega) : x_j \in \mathcal{N}_h^0\}$, and $\mathcal{N}_h^0 \subset \mathcal{N}_h$ is the collection of nodes inside Ω. Taking the time derivative of u_h yields

$$\frac{\partial u_h}{\partial t} = \sum_{x_j \in \mathcal{N}_h} \frac{du_j}{dt} \phi_j^t + \sum_{x_j \in \mathcal{N}_h^{i,t}} u_j \frac{\partial \phi_j^t}{\partial t} + \sum_{T \in \mathcal{T}_h^{i,t}} \frac{dQ}{dt} \phi_J^t + \sum_{T \in \mathcal{T}_h^{i,t}} Q \frac{\partial \phi_J^t}{\partial t}. \tag{2.5}$$

Using (2.3)-(2.5) in the IFE equation above and substituting v_h by the IFE basis functions ϕ_i^t, we obtain an ODE system of $u_j(t)$:

$$\sum_{x_j\in\mathcal{N}_h} u_j'(t)\int_\Omega \phi_i^t\phi_j^t \mathrm{d}x + \sum_{x_j\in\mathcal{N}_{h,t}^i} u_j(t)\int_\Omega \phi_i^t\left(\frac{\partial}{\partial t}\phi_j^t\right)\mathrm{d}x + \sum_{x_j\in\mathcal{N}_h} u_j(t)\int_\Omega \beta\phi_{ix}^t\phi_{jx}^t\mathrm{d}x$$

$$= \int_\Omega f\phi_i^t \mathrm{d}X - Q(\alpha)\phi_i^t(\alpha) - \sum_{T\in\mathcal{T}_h^{i,t}}\int_T \phi_i^t\frac{\partial Q}{\partial t}\phi_J^t\mathrm{d}x - \sum_{T\in\mathcal{T}_h^{i,t}}\int_T \phi_i^t Q\frac{\partial \phi_{J,T}^t}{\partial t}\mathrm{d}x$$

$$- \sum_{T\in\mathcal{T}_h^{i,t}}\int_T \beta\phi_{i,x}^t(Q\phi_{J,x}^t)\mathrm{d}x, \qquad \forall \phi_j^t\in S_h^{t,0}(\Omega). \tag{2.6}$$

The matrix form of this IFE method of lines is as follows:

$$M(t)\mathbf{u}'(t) + (K(t)+A(t))\mathbf{u}(t) = \mathbf{rhs}_f(t) - \mathbf{rhs}_Q(t), \tag{2.7}$$

where

- $M(t)$, $A(t)$ are mass and stiffness matrices associated to the first and third terms on the left hand side of (2.6).
- $K(t)$ is corresponding to the second term on the left hand side of (2.6).
- $\mathbf{rhs}_f(t)$ is the source term vector associated to the first term on the right hand side of (2.6).
- $\mathbf{rhs}_Q(t)$ is related to the last four terms of (2.6).

REMARK 2.1. If we solve a moving interface problem with a homogeneous flux jump condition, *i.e.*, $Q(t)=0$, then $\mathbf{rhs}_Q(t)=\mathbf{0}$ in (2.7); if we solve a problem with a static interface, *i.e.*, $\alpha(t)=\alpha$, then $K(t)=0$ in (2.7).

2.3. Some Implementation Issues. In this subsection, we briefly discuss some implementation issues for the IFE method of lines.

Matrices $M(t)$, $A(t)$ and vector $\mathbf{rhs}_f(t)$: Standard IFE packages developed for the problem with a fixed interface can be directly used to assemble $M(t)$, $A(t)$, and $\mathbf{rhs}_f(t)$. The only thing one needs to pay attention is to update the interface location for a given value of the time variable t in the computation.

Matrix $K(t)$: This matrix involves integrals of the time derivative of IFE basis functions $\frac{\partial\phi_i^t}{\partial t}$. We would like to mention that $K(t)$ is much sparser than $M(t)$ or $A(t)$; hence, it costs little time to get it assembled. The complete procedure for assembling $K(t)$ is provided in [**HLLZ12**].

Vector $\mathbf{rhs}_Q(t)$: The assembling of this vector involves the integrals of ϕ_J^t, $\phi_{J,x}^t$, $\frac{\partial\phi_J^t}{\partial t}$. From (2.1) and (2.2) we can easily obtain

$$\frac{\partial\phi_J^t(x)}{\partial t} = \begin{cases} \dfrac{\beta^+(x_{i+1}-x_i)\alpha'(t)}{(\beta^-(\alpha-x_{i+1})+\beta^+(x_i-\alpha))^2}(x-x_i), & \text{in } T^-,\\ \dfrac{-\beta^-(x_{i+1}-x_i)\alpha'(t)}{(\beta^-(\alpha-x_{i+1})+\beta^+(x_i-\alpha))^2}(x_{i+1}-x), & \text{in } T^+, \end{cases} \tag{2.8}$$

$$\phi_{J,x}(x) = \begin{cases} \dfrac{x_{i+1}-\alpha(t)}{\beta^-(\alpha(t)-x_{i+1})+\beta^+(x_i-\alpha(t))}, & \text{in } T^-,\\ \dfrac{x_i-\alpha(t)}{\beta^-(\alpha(t)-x_{i+1})+\beta^+(x_i-\alpha(t))}, & \text{in } T^+. \end{cases} \tag{2.9}$$

We emphasize again that assembling vector $\mathbf{rhs}_Q(t)$ costs little time. This is because we only need to calculate related integrals locally over the interface element. As a consequence, this vector is also very sparse.

3. Numerical Experiments

In this section, we present numerical examples to demonstrate features of this IFE MoL for solving moving interface problem with a nonhomogeneous flux jump.

We consider the interface problem defined on the solution domain $\Omega \times [0, T_{end}]$, where $\Omega = (0, 1)$ and $T_{end} = 1$. The interface $\alpha(t)$ is a moving point which separates Ω into two sub-domains $\Omega^-(t) = (0, \alpha(t))$ and $\Omega^+ = (\alpha(t), 1)$. The exact solution $u(t, x)$ is chosen as follows

$$u(x,t) = \begin{cases} \left((x-\alpha(t))^2 + \frac{1}{\beta^-}\right) e^x - \frac{1}{\beta^-} e^{\alpha(t)}, & x \in (0, \alpha(t)), \\ \left((x-\alpha(t))^2 + \frac{2}{\beta^+}\right) e^x - \frac{2}{\beta^+} e^{\alpha(t)}, & x \in (\alpha(t), 1). \end{cases} \tag{3.1}$$

Simple calculations show $Q(t) = e^{\alpha(t)} > 0$.

Example 3.1. **General ODE Solver.** In this example, we test some general ODE solvers with fixed time step. We denote the step size by τ, and let $t_n = n\tau$, with $n = 0, 1, \cdots, N$. We assume the moving interface is governed by

$$\alpha(t) = \alpha_1(t) = \left(\frac{\pi}{5} - \frac{1}{3}\right) t + \frac{1}{3}.$$

The ODE system in the IFE MoL (2.7) is equivalent to the standard form:

$$\mathbf{u}' = F(t, \mathbf{u}), \qquad \mathbf{u}(0) = \mathbf{u}_0,$$

where

$$F(t, \mathbf{u}) = M(t)^{-1}\Big(- (K(t) + A(t))\mathbf{u} + \mathbf{rhs}_f(t) - \mathbf{rhs}_Q(t)\Big),$$

and $\mathbf{u}_0 = (u_0(x_j)),\ x_j \in \mathcal{N}_h$. Popular ODE solvers such as Runge Kutta methods and multi-step methods can be employed to solve this ODE system. We have tested several second order ODE solvers in our experiments because they have the order of accuracy comparable to that of the IFE space used in the spacial discretization, and we select $h = \tau$ in these experiments.

Numerical results produced by the implicit midpoint scheme and second order backward difference (BDF) scheme [**AP98**] are listed in Tables 1 and 2. Errors of numerical solutions in L^∞, L^2, and semi-H^1 norms are calculated at the final time level $t = 1$. Linear regression of these errors with different mesh size h yields the convergence order for each Sobolev norm. Both small coefficient jump $(\beta^-, \beta^+) = (1, 3)$, and large coefficient jump $(\beta^-, \beta^+) = (1, 1000)$ are tested.

Table 1. Errors of Linear IFE MoL at $t = 1$ with $\beta^- = 1$, $\beta^+ = 3$

	Implicit Midpoint			BDF2		
h	$\|\cdot\|_{L_\infty}$	$\|\cdot\|_{L_2}$	$\|\cdot\|_{H_1}$	$\|\cdot\|_{L_\infty}$	$\|\cdot\|_{L_2}$	$\|\cdot\|_{H_1}$
1/20	$1.42E{-4}$	$1.20E{-3}$	$7.98E{-2}$	$1.55E{-4}$	$1.23E{-3}$	$7.98E{-2}$
1/40	$3.02E{-5}$	$2.95E{-4}$	$4.06E{-2}$	$4.43E{-5}$	$2.86E{-4}$	$4.06E{-2}$
1/80	$3.95E{-5}$	$8.22E{-5}$	$2.01E{-2}$	$2.31E{-5}$	$7.83E{-5}$	$2.01E{-2}$
1/160	$5.00E{-6}$	$1.98E{-5}$	$1.00E{-2}$	$5.65E{-6}$	$1.97E{-5}$	$1.00E{-2}$
1/320	$3.12E{-6}$	$4.71E{-6}$	$5.02E{-3}$	$4.60E{-6}$	$4.52E{-6}$	$5.02E{-3}$
1/640	$3.86E{-7}$	$1.25E{-6}$	$2.51E{-3}$	$7.06E{-7}$	$1.18E{-6}$	$2.51E{-3}$
1/1280	$3.53E{-7}$	$2.53E{-7}$	$1.25E{-3}$	$1.71E{-7}$	$2.23E{-7}$	$1.25E{-3}$
Order	1.51	2.02	1.00	1.56	2.04	1.00

TABLE 2. Errors of Linear IFE MoL at $t = 1$ with $\beta^- = 1$, $\beta^+ = 1000$

	Implicit Midpoint			BDF2		
h	$\|\cdot\|_{L_\infty}$	$\|\cdot\|_{L_2}$	$\|\cdot\|_{H_1}$	$\|\cdot\|_{L_\infty}$	$\|\cdot\|_{L_2}$	$\|\cdot\|_{H_1}$
1/20	$1.96E{-4}$	$9.68E{-4}$	$6.78E{-2}$	$6.40E{-5}$	$9.96E{-4}$	$6.77E{-2}$
1/40	$7.10E{-5}$	$2.62E{-4}$	$3.81E{-2}$	$2.11E{-5}$	$2.64E{-4}$	$3.81E{-2}$
1/80	$2.00E{-5}$	$6.40E{-5}$	$1.74E{-2}$	$8.79E{-6}$	$6.41E{-5}$	$1.74E{-2}$
1/160	$5.84E{-6}$	$1.55E{-5}$	$8.57E{-3}$	$1.22E{-6}$	$1.57E{-5}$	$8.56E{-3}$
1/320	$2.87E{-6}$	$3.94E{-6}$	$4.45E{-3}$	$8.83E{-7}$	$3.87E{-6}$	$4.45E{-3}$
1/640	$8.94E{-7}$	$9.52E{-7}$	$2.16E{-3}$	$1.68E{-7}$	$9.63E{-7}$	$2.16E{-3}$
1/1280	$2.04E{-7}$	$2.51E{-7}$	$1.07E{-3}$	$4.84E{-8}$	$2.50E{-7}$	$1.07E{-3}$
Order	1.61	2.00	1.01	1.73	2.00	1.01

The data in Table 1 and 2 suggest that errors in L^2 and H^1 norms obey optimal rates. However, errors in L^∞ norm has a sub-optimal convergence order, and the reason for this sub-optimal convergence is an interesting topic for future research. Other ODE solvers such as the Crank-Nicolson, diagonally implicit Runge Kutta (DIRK2) schemes, etc., are also tested. The performances are similar, so we omit the corresponding data in this manuscript.

EXAMPLE 3.2. **Adaptive ODE Solver.** One attractive feature of the method of lines is that the adaptivity in time variable can be easily realized. Hence, with a suitably chosen adaptive ODE solver, the IFE MoL can efficiently produce a reliable numerical solution to a parabolic initial boundary value problem whose interface changes with respect to time at a variable rate.

To demonstrate this feature, we consider another example which is basically the same as that in the previous example but its interface is governed by:

$$\alpha(t) = \alpha_2(t) = \frac{1}{30}\left(\log(10t + 0.25) + \frac{1}{500}e^{6t+3} + 4\right).$$

Obviously, this interface function changes with respect to time at a variable rate, see the plot on the left in Figure 1. We use the standard embedded DIRK45 scheme in [**HW96**] to solve these two moving interface problems. The plot on the right in Figure 1 displays the time step sizes used for producing a numerical solution to the second moving interface problem. Comparing this plot with the derivative of $\alpha(t)$ in the plot on the left, we can see that our IFE MoL with this adaptive ODE solver uses larger time step sizes in the region where $|\alpha'(t)|$ has smaller values while it uses smaller time step sizes in the region where $|\alpha'(t)|$ is large. This obviously indicates that this IFE MoL can efficiently handle the change of the interface with respect to time via the adaptivity feature in DIRK45.

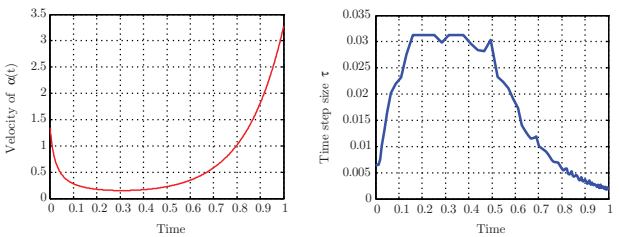

FIGURE 1. left plot: the graph of $|\alpha'(t)|$; right plot: time step sizes used in the adaptive IFE MoL on a uniform mesh with $h = 1/160$.

As demonstrated by the data in Table 3, this adaptive feature enables the IFE MoL to produce reliable numerical results by strategically choosing the step size in the time integration. The mesh sizes used in this group of numerical experiments are listed in the first column of Table 3. The second and third columns contain error data of the IFE solutions to the two moving interface problems. The numbers below N are the total numbers of time iterations. We note that the interface in the second moving interface problem changes more complicatedly than the first. Consequently, the adaptive IFE MoL uses less time iterations for the first problem. More importantly, applying linear regression to the data in this table, we can see that the adaptive IFE MoL produces numerical solutions to both problems with optimal convergence rates in the L^2 and H^1 norms.

Figure 2 displays the curve for the L^∞ norm errors in the IFE MoL solution generated on a mesh of $h = 1/160$ with an adaptive ODE solver at a sequence of time levels. This adaptive IFE MoL solution uses 108 time steps. The other two curves are for L^∞ norm errors in numerical solutions produced by IFE methods with a uniform time step size $\tau = 1/108$. It is clear that the adaptive IFE MoL can maintain the error in its solution below a certain level almost uniformly over the whole time interval while errors in those IFE methods based a uniform time step size grow along with the time. These numerical results further demonstrate the reliability of the IFE MoL combined with a good adaptive ODE solver.

TABLE 3. Errors of Adaptive DIRK45 at $t = 1$ with $\beta^- = 1$, $\beta^+ = 1000$

	DIRK45: $\alpha(t) = \alpha_1(t)$				DIRK45: $\alpha(t) = \alpha_2(t)$			
h	N	$\|\cdot\|_{L_\infty}$	$\|\cdot\|_{L_2}$	$\|\cdot\|_{H_1}$	N	$\|\cdot\|_{L_\infty}$	$\|\cdot\|_{L_2}$	$\|\cdot\|_{H_1}$
1/20	8	$3.27E{-5}$	$9.87E{-4}$	$6.77E{-2}$	16	$2.27E{-3}$	$1.98E{-3}$	$1.68E{-1}$
1/40	13	$1.42E{-5}$	$2.66E{-4}$	$3.81E{-2}$	30	$6.85E{-4}$	$5.31E{-4}$	$4.90E{-2}$
1/80	25	$2.60E{-6}$	$6.35E{-5}$	$1.74E{-2}$	57	$1.13E{-4}$	$1.03E{-4}$	$1.76E{-2}$
1/160	49	$1.09E{-6}$	$1.58E{-5}$	$8.56E{-3}$	108	$3.10E{-5}$	$2.89E{-5}$	$7.74E{-3}$
1/320	95	$8.01E{-7}$	$4.03E{-6}$	$4.45E{-3}$	217	$2.22E{-5}$	$9.13E{-6}$	$3.76E{-3}$
1/640	190	$2.59E{-7}$	$1.04E{-6}$	$2.16E{-3}$	432	$3.99E{-6}$	$2.29E{-6}$	$1.88E{-3}$
1/1280	379	$7.86E{-8}$	$2.68E{-7}$	$1.07E{-3}$	864	$8.45E{-7}$	$6.32E{-7}$	$9.38E{-4}$
Order		1.41	1.98	1.01		1.83	1.93	1.22

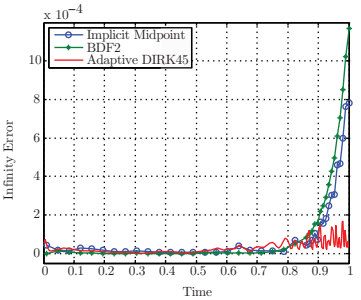

FIGURE 2. Curves for L^∞ errors of IFE solutions generated on a uniform mesh with $h = 1/160$. The adaptive IFE MoL uses 108 times steps determined according to error control strategy, but the other two IFE methods use a uniform time step size $\tau = 1/108$.

4. Conclusion

In this article, we develop an IFE MoL for the one dimensional parabolic moving interface problem with a nonhomogeneous flux jump condition. An enrichment linear IFE function is constructed to homogenize the original problem. Abundant choice of efficient ODE solvers allows this IFE MoL to solve this kind of moving interface problems efficiently.

References

[AL09] S. Adjerid and T. Lin, *A p-th degree immersed finite element for boundary value problems with discontinuous coefficients*, Appl. Numer. Math. **59** (2009), no. 6, 1303–1321. MR2510495 (2009m:65123)

[AP98] U. Ascher and L. Petzold, *Computer methods for ordinary differential equations and differential-algebraic equations*, Society for Industrial and Applied Mathematics (SIAM), Philadelphia, PA, 1998. MR1638643 (99k:65052)

[CDH67] J. Cannon, J. Douglas, and C. Hill, *A multi-boundary Stefan problem and the disappearance of phases*, J. Math. Mech. **17** (1967), 21–33. MR0269999 (42:4892)

[Coo75] D. Cook, *The theory of electromagnetic field*, Prentice-Hall Physics Series, Prentice Hall College Div, 1975.

[GLL07] Y. Gong, B. Li, and Z. Li, *Immersed-interface finite-element methods for elliptic interface problems with nonhomogeneous jump conditions*, SIAM J. Numer. Anal. **46** (2007), no. 1, 472–495. MR2377272 (2008m:65319)

[He09] X. He, *Bilinear immersed finite elements for interface problems*, Ph.D. thesis, Virginia Tech, 2009.

[HLL11] X. He, T. Lin, and Y. Lin, *Immersed finite element methods for elliptic interface problems with non-homogeneous jump conditions*, Int. J. Numer. Anal. Model. **8** (2011), no. 2, 284–301. MR2740492 (2011h:65224)

[HLLZ12] X. He, T. Lin, Y. Lin, and X. Zhang, *Immersed finite element methods for parabolic equations with moving interface*, Numer. Methods Partial Differential Equations (2012), to appear.

[HW96] E. Hairer and G. Wanner, *Solving ordinary differential equations*, Springer Series in Computational Mathematics, 14, vol. II, Springer-Verlag, Berlin, 1996. MR1439506 (97m:65007)

[LLLR04] Z. Li, T. Lin, Y. Lin, and R. Rogers, *An immersed finite element space and its approximation capability*, Numer. Methods Partial Differential Equations **20** (2004), no. 3, 338–367. MR2046521 (2005f:65153)

[LLW03] Z. Li, T. Lin, and X. Wu, *New cartesian grid methods for interface problems using the finite element formulation*, Numer. Math. **96** (2003), no. 1, 61–98. MR2018791 (2005c:65104)

[LLZ12] T. Lin, Y. Lin, and X. Zhang, *A method of lines based on immersed finite elements for parabolic moving interface problems*, Adv. Appl. Math. Mech. (2012), to appear.

[Miy06] T. Miyazaki, *Water flow in soils*, CRC Press, 2006.

[WLL11] C. Wu, Z. Li, and M. Lai, *Adaptive mesh refinement for elliptic interface problems using the non-conforming immersed finite element method*, Int. J. Numer. Anal. Model. **8** (2011), no. 3, 466–483. MR2805671 (2012g:65267)

[WWY12] K. Wang, H. Wang, and X. Yu, *An immersed Eulerian-Lagrangian localized adjoint method for transient advection-diffusion equations with interfaces*, Int. J. Numer. Anal. Model. **9** (2012), no. 1, 29–42. MR2871300 (2012k:65118)

[XLQ11] H. Xie, Z. Li, and Z. Qiao, *A finite element method for elasticity interface problems with locally modified triangulations*, Int. J. Numer. Anal. Model. **8** (2011), no. 2, 189–200. MR2740487 (2011h:74113)

[ZS11] Q. Zhang and W. Sun, *A numerical study of air-vapor-heat transport through textile materials with a moving interface*, J. Comput. Appl. Math. **236** (2011), no. 5, 819–833. MR2853507

Department of Mathematics, Virginia Tech, Blacksburg, Virginia 24061
E-mail address: tlin@vt.edu

Department of Applied Mathematics, Hong Kong Polytechnic University, Hung Hom, Hong Kong, and Department of Mathematical and Statistics Science, University of Alberta, Edmonton AB, T6G 2G1, Canada
E-mail address: malin@polyu.edu.hk and yanlin@ualberta.ca

Department of Mathematics, Virginia Tech, Blacksburg, Virginia 24061
E-mail address: xuz@vt.edu